Detecting anomalous phase synchronization from time series

Isao T. Tokuda,[1] Syamal Kumar Dana,[2] and Jürgen Kurths[3]
[1]*School of Information Science, Japan Advanced Institute of Science and Technology, Ishikawa 923-1292, Japan*
[2]*Instrument Division, India Institute of Chemical Biology, Jadavpur, Kolkata 700032, India*
[3]*Department of Physics, Humboldt University Berlin, 12489 Berlin, Germany and Potsdam Institute for Climate Impact Research, 14473 Potsdam, Gernany*

(Received 7 December 2007; accepted 22 May 2008; published online 30 June 2008)

Modeling approaches are presented for detecting an anomalous route to phase synchronization from time series of two interacting nonlinear oscillators. The anomalous transition is characterized by an enlargement of the mean frequency difference between the oscillators with an initial increase in the coupling strength. Although such a structure is common in a large class of coupled nonisochronous oscillators, prediction of the anomalous transition is nontrivial for experimental systems, whose dynamical properties are unknown. Two approaches are examined; one is a phase equational modeling of coupled limit cycle oscillators and the other is a nonlinear predictive modeling of coupled chaotic oscillators. Application to prototypical models such as two interacting predator-prey systems in both limit cycle and chaotic regimes demonstrates the capability of detecting the anomalous structure from only a few sets of time series. Experimental data from two coupled Chua circuits shows its applicability to real experimental system. © *2008 American Institute of Physics*.
[DOI: 10.1063/1.2943308]

The collective behavior of a population of interacting rhythmic oscillators has attracted significant attention in many areas of science and technology over the last decades. Synchronization is one of the most fundamental phenomena in such systems, where dynamical patterns of the oscillatory elements are entrained through the mutual coupling. In a large class of coupled nonlinear systems in the real world, which typically creates heterogeneity such as frequency mismatch among the oscillators, phase synchronization has been found to be quite a common phenomenon in which, despite some variability in the amplitude, the phase of the oscillators is locked. Transition from disordered state to phase synchronization is usually expected to be a monotonic process, where a gradual increase in the coupling strength monotonically decreases the frequency difference among the oscillators. However, due to nonisochronous property of the nonlinear oscillators as well as asymmetry in the coupling, it has been recently shown that the increased coupling can initially increase the frequency difference and then eventually decreases it into zero. This nonmonotonic route is called "anomalous phase synchronization," which is commonly found in a variety of systems including biological networks. Given a time series measured from such oscillators, the next important problem is to retrieve the anomalous structure hidden behind the measurement. This provides a nontrivial situation, since the underlying coupled dynamics is usually not known. This paper presents unique modeling approaches to detect the anomalous phase synchronization from time series. Based only on a few measurements, nonmonotonic transition to synchronization can be well detected for two coupled limit cycle oscillators as well as two coupled chaotic oscillators. This enables the prediction of the onset point of the synchronization, thus providing an important application to real experimental systems.

I. INTRODUCTION

Synchronization is a ubiquitous phenomenon of coupled nonlinear oscillations found in many fields of science and engineering.[1–3] In real-world systems, the oscillatory elements are inherently nonidentical, where individual oscillator is governed by a different natural frequency. Such a frequency mismatch can be tuned to zero by introducing an interaction among the oscillators, which induces a phase synchronization (PS). Due to this natural problem formulation, the PS has been attracting a great deal of attention. An earlier and yet famous example is the weakly coupled limit cycle oscillators, whose dynamics can be reduced to a system of interacting phase oscillators.[2] The coupling induced synchrony, known as the Kuramoto transition, provides a simple description of PS. The idea of PS has been extended to the study of coupled chaotic oscillators.[4] With an adequate definition of phase, it has been shown that the phase of chaotic oscillators can be entrained through coupling, where the amplitude of each oscillator is still independent and chaotic. Such chaotic phase synchronization can be found in a variety of laboratory experiments as well as natural systems.[5,6]

It is usual that increase in the coupling strength induces a monotonic decrease in the mean frequency difference between the nonlinear oscillators, leading to PS. In contrast to such a monotonic transition, a new route to PS has been recently found, where a small coupling initially enlarges the frequency difference and then PS sets in later for a larger coupling strength.[7] The underlying mechanism of this "anomalous" phase synchronization (APS) has been clarified

as a nonisochronicity of the nonlinear oscillator, whereas asymmetry of the coupling is also known to pronounce the anomalous structure. The APS can be seen in a large class of systems including coupled limit cycle oscillators as well as coupled chaotic oscillators.[8] Experiments with two coupled Chua circuits also provides a clear laboratory example.[9,10]

To analyze the experimental data from such coupled oscillators, special techniques of synchronization analysis should be developed. Although conventional techniques are shown to be very efficient for detecting PS even for noisy and nonstationary data,[3,11–14] only a few deal with the problem of modeling the coupled oscillators from time series data. Such a model would reconstruct the synchronization diagram that classifies the parameter space of the coupling strength into regions of PS and non-PS. Of special interest in this modeling is to detect the anomalous structure, which is usually hidden behind the time series data. This is a challenging problem, since the anomalous structure can mislead the modeling to provide a wrong prediction on the onset point of the PS. Hence, the aim of this paper is to present modeling techniques for reconstructing the anomalous structure of coupled oscillators. We deal with both coupled limit cycle oscillators and coupled chaotic oscillators. For simplicity, we restrict ourselves to the case of two interacting oscillators.

Our study is based upon two approaches. The first one is a phase equational modeling of coupled limit cycle oscillators. The second one is a nonlinear modeling technique of coupled chaotic oscillators. By using simulation data from prototypical models of APS as well as experimental data from two coupled Chua circuits, we demonstrate the modeling power of detecting the anomalous structure only from a few sets of measurement data.

The present paper is organized as follows. In Sec. II, phase equational modeling is introduced to coupled limit cycles. Simulation results with two interacting limit cycle predator-prey model are presented. In Sec. III, nonlinear modeling is applied to coupled chaotic oscillators. Results with simulation data from two interacting chaotic predator-prey systems as well as experimental data from two coupled Chua circuits are presented. Section IV is devoted for conclusions and discussions.

II. COUPLED LIMIT CYCLES

A. Problem and method

We start with a system of two weakly coupled nearly identical limit cycle oscillators,

$$\dot{x}_{1,2} = F_{1,2}(x_{1,2}) + CJ_{1,2}(x_{1,2}, x_{2,1}), \tag{1}$$

where x_i ($\in R^m$) and F_i represent state variables and dynamics of the first oscillator ($i=1$) and the second oscillator ($i=2$), C and J_i are the coupling constant and the interaction function between both oscillators. The interaction is considered to be asymmetric; i.e., $J_1 \neq J_2$. With an increase in C, the system is assumed to give rise to APS.

As a recording condition, we assume that simultaneous measurements of the two oscillators are made as $\{\xi_1(n\Delta t), \xi_2(n\Delta t) : n=1, \ldots, N\}$, where each variable is observed through a function $G: R^m \to R^1$ as $\xi_i(t) = G(x_i(t))$ with a sampling interval of Δt. Our objective is to reconstruct the synchronization diagram including the anomalous structure from the measurement data. Our main conditions are (i) the underlying dynamics (1) is unknown, (ii) the coupling constant C associated with the measured data is taken from a nonsynchronous regime, and (iii) the coupling type is known to be diffusive.

Our approach is based upon the modeling technique recently introduced to extract phase equations from multivariate time series of a population of coupled limit cycle oscillators.[15] According to the phase reduction theory,[2] if the coupling C is weak and if the coupled limit cycle oscillators have similar natural frequencies ω_i, the system dynamics (1) can be reduced to phase equations of the following form:

$$\dot{\theta}_{1,2} = \omega_{1,2} + CH_{1,2}(\theta_{2,1} - \theta_{1,2}). \tag{2}$$

Our strategy is to infer the above phase equations (2) from the measurement data according to the following steps so that the obtained phase models can be utilized to reconstruct the synchronization diagram of the original system (1).

(A1) Determine phases $\theta_{1,2}(t)$ from data $\xi_{1,2}(t)$. Among various definitions of phases,[3] a simple formula is appropriate here, where the phase θ is increased by 2π at every local maximum of $\xi(t)$ and between the local maxima the phase grows linearly in proportion to time.

(A2) Fit the phases $\theta_{1,2}(t)$ to the phase equations:

$$\dot{\theta}_{1,2} = \omega_{1,2} + C\tilde{H}_{1,2}(\theta_{2,1} - \theta_{1,2}), \tag{3}$$

$$\tilde{H}_i(\Delta\theta) = \sum_{j=1}^{\mu} a_{ij} \sin j\Delta\theta + b_{ij}(\cos j\Delta\theta - 1), \tag{4}$$

by estimating the unknown parameters $p = \{\omega_i, a_{ij}, b_{ij}\}$ via the multiple-shooting method.[16] Note that the interaction function H_i, which is in general nonlinear and periodic with respect to 2π, is approximated by a Fourier expansion up to order of μ. [For simplicity, we consider difference coupling. Thus, the interaction function is set to zero for zero phase difference; i.e., $\tilde{H}_i(0)=0$.] In the multiple-shooting, we denote the time evolution of the phase equations (3) and (4) with respect to the initial condition $\theta_{1,2}(0)$ by $\theta_{1,2}(t) = \phi^t_{1,2}(\theta_{1,2}(0), \theta_{2,1}(0), p)$. Taking the phases $\theta_{1,2}(t)$ at each sampling time $t=i\Delta t$ as the initial condition, the phase equations must satisfy the following boundary conditions at the next sampling step $t=(i+1)\Delta t$:

$$\theta_{1,2}((n+1)\Delta t) = \phi^{\Delta t}_{1,2}(\theta_{1,2}(n\Delta t), \theta_{2,1}(n\Delta t), p). \tag{5}$$

With respect to the unknown parameters p, we solve the above nonlinear equations by the generalized Newton method. The evolution function $\phi^t_{1,2}$ is integrated numerically. For the computation of the gradients $\partial\phi_{1,2}/\partial p$, which are needed for the Newton method, variational equations of the phase equations (3) and (4) are also solved numerically.

(A3) To avoid the overfitting problem, a cross-validation technique[17] is utilized to determine the optimum number μ of the higher harmonics in the interaction function. We divide the measurement data into two parts. For the first half of the data $\{\theta_{1,2}(n\Delta t): n=1,\ldots,N/2\}$, which is used as the training sample, the parameter values p are estimated. We then apply the estimated parameters to the latter half data $\{\theta_{1,2}(n\Delta t): n=1+N/2,\ldots,N\}$, which is used as the test sample, and measure the error

$$E_c = (1/N)\sum_{n=N/2}^{N-1}\sum_{i=1}^{2}\left|\theta_i((n+1)\Delta t) - \phi_i^{\Delta t}(\theta_i(n\Delta t),\theta_{i+1}(n\Delta t),p)\right|.$$

The order number μ that provides the minimum error is considered to be the optimum.

(A4) By simulating the obtained phase equations (3) and (4), compute the normalized frequency difference as $\Delta\omega = 2|\bar{\omega}_1-\bar{\omega}_2|/(\bar{\omega}_1+\bar{\omega}_2)$ ($\bar{\omega}_{1,2}$: frequency of the first and second oscillator in the presence of coupling). The synchronization diagram is drawn by plotting $\Delta\omega$, which depends upon the coupling strength C.

B. Application

As a prototypical example of coupled limit cycle oscillators, we consider the following two interacting predator-prey systems:[8]

$$\dot{x}_{1,2} = -ax_{1,2}\left(1-\frac{x_{1,2}}{K}\right) - \alpha\frac{x_{1,2}y_{1,2}}{1+\kappa x_{1,2}}, \tag{6}$$

$$\dot{y}_{1,2} = -b_{1,2}y_{1,2} + \alpha\frac{x_{1,2}y_{1,2}}{1+\kappa x_{1,2}} + C_{1,2}(y_{2,1}-y_{1,2}). \tag{7}$$

x_i and y_i denote the prey and predator species, respectively, a and b are the birth and death rates, respectively, K is the prey carrying capacity, α is the predation rate, and κ corresponds to the half-saturation constant of the functional response. The parameter values are set as $a=1$, $\alpha=3$, $K=3$, $\kappa=1$, where the mismatched parameters are chosen as $b_1=0.995$ and $b_2=1$. For sufficiently large K, each predator-prey system is well known to exhibit limit cycle oscillations.

Figure 2(a) shows interaction functions $H_{1,2}(\Delta\theta)$ of the two limit cycle oscillators, obtained by applying a perturbation method to the original equations (6) and (7). The perturbation method is the standard method to estimate the interaction function based upon the convolution of the phase response curve with the external stimuli.[2,18,19] This approach cannot be applied directly to the present problem formulation, since it requires the phase response curve, which should be obtained by applying external perturbations to each nonlinear oscillator in an isolated condition. The first-order Fourier approximation of the estimated interaction functions yields $H_1(\Delta\theta)\approx 0.45\sin\Delta\theta + 3.4(1-\cos\Delta\theta)$ and $H_2(\Delta\theta)\approx 0.52\sin\Delta\theta + 4.05(1-\cos\Delta\theta)$. This indicates that the interaction functions have a very strong cosine-component. Due to this nonisochronicity, the coupled limit cycles system of equations (6) and (7) exhibits APS. In order to further pronounce the anomalous structure, asymmetry is introduced to the coupling as $C_{1,2}=C(1\mp\chi)$ with a control parameter $\chi=0.1$.

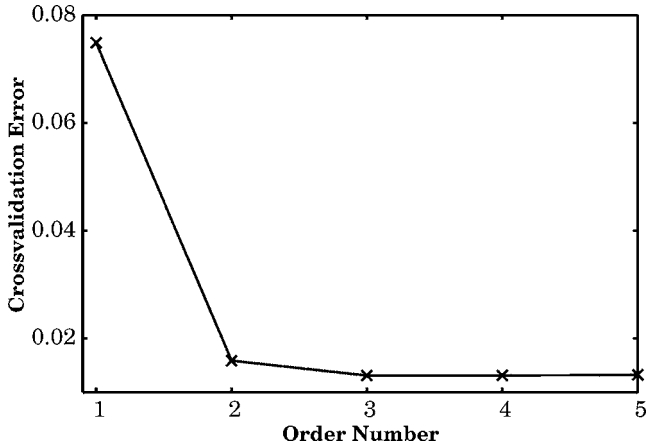

FIG. 1. Cross-validation test applied to coupled limit cycle predator-prey model. For order number $\mu=1,2,\ldots,5$, error function E_c is computed for the test data, which are not used for the parameter estimation. The minimum error points the optimum Fourier order at $\mu=3$.

As a measurement of these coupled limit cycle oscillators, bivariate data were recorded as $\{x_1(t),x_2(t)\}$ under the coupling strength of $C=0.001$, which is within nonsynchronized regime (see Fig. 3). The sampling interval was set to be $\Delta t=0.08$ for the extraction of the phase $\{\theta_i(t)\}$. To apply the multiple-shooting method, the data have been downsampled to $\Delta t=1000\times 0.08$ and the total of $N=2400$ data points have been collected for the parameter estimation.

In the multiple-shooting, initially, the unknown parameter values were all set to be zero; i.e., $\omega_i=0$, $a_{ij}=b_{ij}=0$. The convergence property was excellent; within 10 Newton steps a good estimate was reached.

Figure 1 shows the result of the cross-validation test, which indicates that the optimum Fourier order is $\mu=3$. For this optimum order, the natural frequencies were estimated as $\omega_1=0.510$ and $\omega_2=0.512$, which are very similar to the values of $\omega_1=0.519$ and $\omega_2=0.521$ obtained by simulating the original equations (6) and (7) in an isolated condition. Figure 2(b) shows the interaction functions $\tilde{H}_{1,2}(\Delta\theta)$ estimated by the present technique. The estimated interaction functions are quite similar to those obtained by the perturbation method as shown in Fig. 2(a). The first-order terms yield $\tilde{H}_1(\Delta\theta)\approx 0.65\sin\Delta\theta + 4.7(1-\cos\Delta\theta)$ and $\tilde{H}_2(\Delta\theta)\approx 1.1\sin\Delta\theta + 5.6(1-\cos\Delta\theta)$, indicating a strong cosine-component (723% and 509% of sine-component), which are in a very good agreement with the estimates obtained by the perturbation method (756% and 779% of sine-component). Furthermore, the coupling asymmetry between the two oscillators was derived as $\max|\tilde{H}_1|/\max|\tilde{H}_2|=0.829$, which is again quite similar to $\max|H_1|/\max|H_2|=0.832$, obtained by the perturbation method.

One of the most important capabilities of the phase modeling is its predictability of the synchronization structure of the original coupled system. By simulating the estimated phase equations (3) and (4), the synchronization diagram has

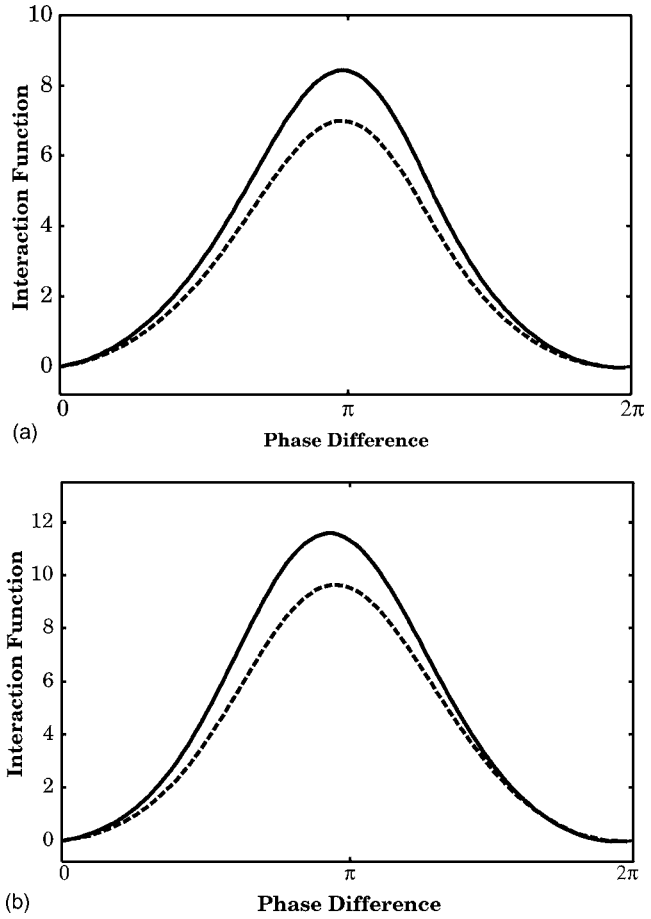

FIG. 2. Interaction function of limit cycle predator-prey model is drawn for the first oscillator $\tilde{H}_1(\Delta\theta)$ (solid line) and for the second oscillator $\tilde{H}_2(\Delta\theta)$ (dotted line). (a) The estimates based upon the perturbation method and (b) estimates based upon the present method.

been drawn by plotting the normalized frequency difference $\Delta\omega$ against the coupling strength C. Figure 3 shows that the synchronization diagram of the phase model produces a structure almost identical to the one obtained by simulating

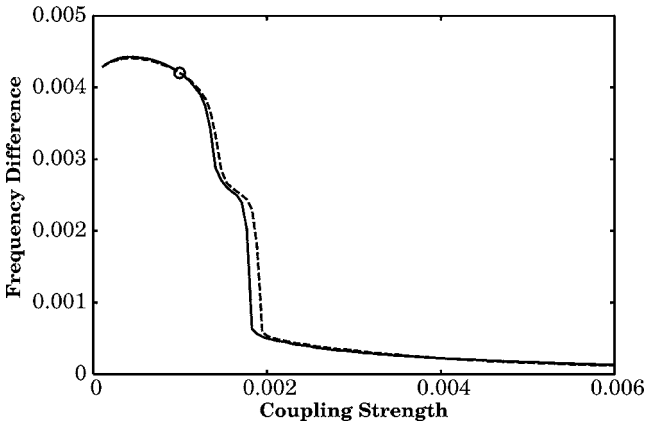

FIG. 3. Synchronization diagram of two coupled limit cycle predator-prey model. Normalized mean frequency difference $\Delta\omega$ is plotted against the coupling strength C. The model prediction (dotted line) is compared with the simulation curve (solid line), which is drawn by using the original Eqs. (6) and (7). The circle marker corresponds to the coupling strength $C=0.001$ utilized for the model estimation.

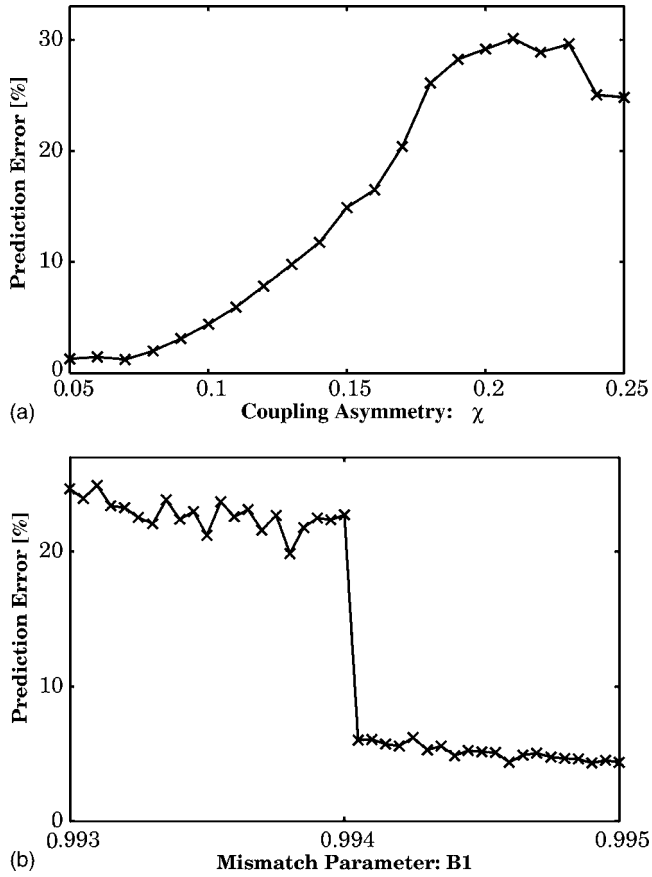

FIG. 4. Dependence of the prediction error E_p of the synchronization diagram on the parameters b_1 and χ. (a) $b_1=0.995$, $b_2=1$, $\chi\in[0.05,0.25]$. (b) $b_1\in[0.993,0.995]$, $b_2=1$, $\chi=0.1$.

the original equations (6) and (7). It should be emphasized that the anomalous property is well reproduced and furthermore the onset point of PS is also precisely predicted by the phase model. Considering the fact that only a single data set was used for this model estimation, the substantial power of the phase modeling approach to the coupled limit cycle oscillators is demonstrated by the present example.

It is important to note that the result of predicting the synchronization depends upon the parameter mismatch $|b_1-b_2|$ and the coupling asymmetry χ, which determine the amount of anomalous property. Figure 4 shows dependence of the prediction error of the synchronization diagram on the parameters b_1 and χ. The prediction error is measured by the deviation of the model diagram from the real diagram as $E_p=100\int_0^{0.006}|\Delta\omega_p(C)-\Delta\omega_o(C)|dC/\int_0^{0.006}|\Delta\omega_o(C)|dC$ [%], where $\Delta\omega_p$ and $\Delta\omega_o$ correspond to normalized frequency difference of phase model and original system, respectively. As the asymmetry parameter χ is increased [in Fig. 4(a)] or as the parameter mismatch $|b_1-b_2|$ is increased [in Fig. 4(b)], the prediction error is also increased. This implies that as the anomalous structure is more pronounced it becomes harder to predict the synchronization diagram. This might be due to the limitation of the phase modeling, where stronger nonlinearity starts to play an important role in the more pronounced APS. The phase modeling should be employed under the condition that the anomalous property is moderate.

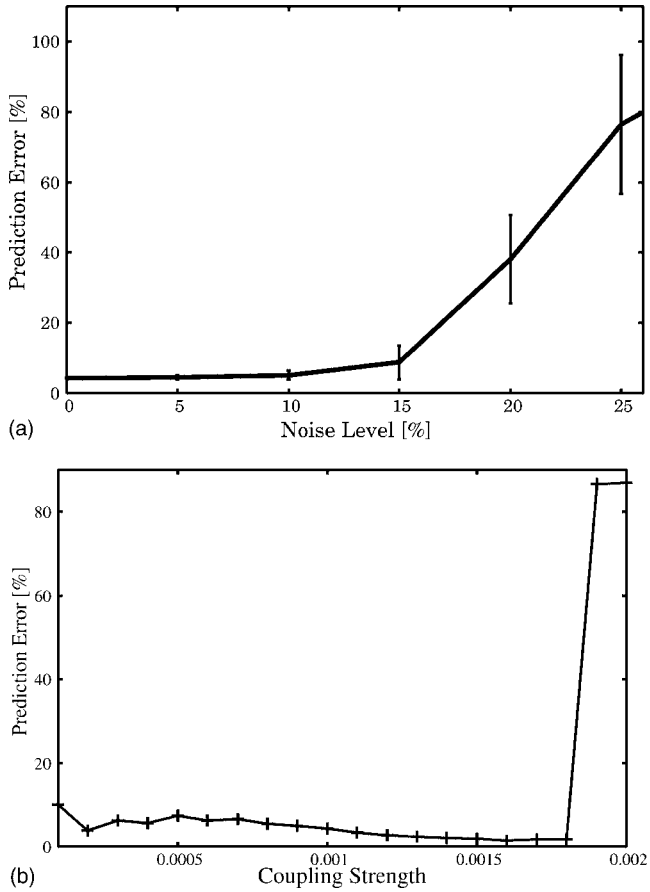

FIG. 5. Dependence of the prediction error E_p on (a) observational noise (from 0% to 25%) and (b) coupling strength $C \in [0, 0.002]$ used for generating the time series. The parameters are set to $(b_1, b_2, \chi) = (0.995, 1, 0.1)$.

Another important issue is the effect of noise, which is inherent in all experimental or natural systems. To study the influence of noise on the estimation results, zero-mean Gaussian noise was added to the bivariate data $\{x_1(t), x_2(t)\}$ as observational noise. The system parameters were set to $(b_1, b_2, \chi) = (0.995, 1, 0.1)$. To reduce the noise effect, a moving average filter, $x_i'(n\Delta t) = (1/20)\Sigma_{j=1}^{20} x_i((n+j)\Delta t)$ $(i=1,2)$, was applied before the phase extraction procedure (A1). Figure 5(a) shows the dependence of the prediction error E_p on the noise level. As the noise level is increased, the prediction error is increased as well. However, up to the noise level of 15%, the model prediction is still very accurate within the error of $E_p < 9\%$. This demonstrates the robustness of the present approach against the observational noise.

Finally, Fig. 5(b) shows the dependence of the prediction error E_p on the coupling strength C used for generating the times series. As the coupling strength is increased, the prediction error is also increased. The reason for this is as follows. As the coupling strength comes close to the onset point of synchronization, the phase difference between the two oscillators may grow extremely slowly. In order for precise estimation of the interaction function, time series that contains enough information on the developmental process of the phase difference is necessary, since the interacting information is contained in such interval. Close to the onset point, however, only a limited information is included, which may cause inaccurate estimation of the interaction function. In this sense, the measurement data away from the onset point is desired for the present technique.

III. COUPLED CHAOTIC OSCILLATORS

A. Problem and method

Let us consider the case of coupled chaotic oscillators. In a manner similar to Sec. II, two diffusively coupled nonlinear oscillators are formulated as

$$\dot{x}_{1,2} = F_{1,2}(x_{1,2}) + C(x_{2,1} - x_{1,2}). \tag{8}$$

From both oscillators, bivariate data $\{\xi_1(n\Delta t), \xi_2(n\Delta t) : n = 1, \ldots, N\}$ are simultaneously measured. The main differences from the assumptions made in the previous section II are: (1) without coupling $(C=0)$, each oscillator $F_{1,2}$ generates a phase-coherent chaos; (2) we assume that the coupling type is known to be a mutual difference coupling $(x_{2,1} - x_{1,2})$; (3) under M conditions associated with different coupling strength C_i $(i=1, \ldots, M)$ in nonsynchronized regime, the bivariate data are obtained. With an increase in C, the system is again assumed to give rise to APS.

Our objective is to reconstruct the synchronization diagram including the anomalous structure from the few data sets. Unlike the previous section, the phase reduction technique[2] cannot be applied to the chaotic PS. Instead, nonlinear modeling technique based on Refs. 20 and 21 is applied to the present case as follows.

First, we embed the bivariate time series $\{\xi_1(t), \xi_2(t)\}$ into delay coordinates

$$X_1(t) = \{\xi_1(t), \xi_1(t-\tau), \ldots, \xi_1(t-(d-1)\tau)\},$$

$$X_2(t) = \{\xi_2(t), \xi_2(t-\tau), \ldots, \xi_2(t-(d-1)\tau)\}$$

(d: embedding dimension, τ: time lag) and suppose according to the embedding theorem[22,23] that there exists the following dynamics:

$$\dot{X}_{1,2}(t) = F_{1,2}(X_{1,2}(t), C(X_{2,1}(t) - X_{1,2}(t))). \tag{9}$$

The main point of our modeling is to construct a set of nonlinear functions $\tilde{F}_{1,2}$, which approximate $F_{1,2}$ in Eq. (9). If the original dynamics (8) is well embedded in the delay coordinate space and the embedded dynamics (9) is precisely modeled, synchronization structure of the original dynamics can be predicted by studying the model equations $\tilde{F}_{1,2}$. For the construction of the nonlinear models $\tilde{F}_{1,2}$, there exist mainly two approaches: local modeling and global modeling. The local approach is to divide the state space into small regions and construct a linear or nonlinear function in each region.[24] The global approach, on the other hand, yields a single nonlinear function that approximates the global dynamics without dividing the space.[25,26] Although the local approach is capable of a precise modeling of the local dynamics, it is not suitable for modeling the global dynamical structure such as bifurcations[26] due to its local property. We therefore take the global approach. Among the global functional systems such as polynomial functions[25] and radial basis functions,[26] an artificial neural network[27] is exploited in

this study. Our modeling procedure consists of the following main steps.

(B1) The embedding dimension d and the time lag τ are chosen. To determine τ, the first zero-crossing point of the autocorrelation function, which is commonly used for the nonlinear data analysis,[28] is exploited. The embedding dimension d can be determined by conventional techniques such as the false nearest neighbor algorithm.[29]

(B2) Each nonlinear function $\tilde{F}_i : R^d \times R^d \to R^d$ $(i=1,2)$ is realized by a three-layer feed-forward neural network,[27] having $2d$-units in the input layer, d-units in the output layer, and h-units in the middle layer. Each neural network has $4dh$ parameters, denoted as W, which are optimized to fit into the data as follows. First, the cost function is defined as

$$E_n(W) = \sum_{i=1}^{M} \sum_{j=1}^{2} \sum_{n=1}^{N-S} \sum_{s=1}^{S} |X_j((n+s)\Delta t, C_i) - \tilde{X}_j((n+s)\Delta t, C_i)|^2, \tag{10}$$

where $\tilde{X}_j$ is the trajectory generated from the model equations

$$\dot{\tilde{X}}_{1,2}(t) = \tilde{F}_{1,2}(\tilde{X}_{1,2}(t), C(\tilde{X}_{2,1}(t) - \tilde{X}_{1,2}(t))) \tag{11}$$

started from the initial condition $\tilde{X}_{1,2}(n\Delta t) = X_{1,2}(n\Delta t)$. Note that the data $X_{1,2}$ and the model trajectories $\tilde{X}_{1,2}$ in Eq. (10) are dependent upon the coupling strength C, since we assume that several data sets are recorded with different coupling conditions. The maximal iteration step is set as $S=5$. To minimize the cost function, the quasi-Newton method based upon the Broyden–Fletcher–Goldfarb–Shanno formula with Luenberger's self-scaling[30] is utilized. To compute the first derivatives of the cost function, variational equations of the model equations (11) are numerically integrated.

(B3) It has been known that the modeling of the coupled system based on a single realization of the nonlinear function $\tilde{F}_{1,2}$ is rather sensitive to the parameter estimation. To overcome this problem, an ensemble technique is utilized.[31] In this technique, Q sets of different nonlinear models $\tilde{F}_{1,2}^{(i)}$ $(i=1,\ldots,Q)$ are collected, each of which can be obtained by the same procedure as (B2) except that a different initial condition, which is generated randomly, is set for the parameter estimation. This results in Q sets of neural networks with the same architecture with different parameter values W. An ensemble average is then taken as $\bar{F}_{1,2} = (1/Q)\Sigma_{i=1}^{Q} \tilde{F}_{1,2}^{(i)}$. It has been shown that this ensemble average is much less sensitive to the model selection, thus provides a highly reliable modeling.[31]

(B4) Mean frequencies of both oscillators $\omega_{1,2}$ can be computed by the free-running of the ensemble model $\dot{X}_{1,2}(t) = \bar{F}_{1,2}(X_{1,2}(t), C(X_{2,1}(t) - X_{1,2}(t)))$. A unit phase of 2π is defined as a duration between one local maximum of the first component of X and the following one. By counting the number N_i of the local maxima during a period T_f, the mean frequency of the ith oscillator can be computed as $\omega_i = 2\pi N_i / T_f$. Normalized mean frequency difference between the two oscillators is then given as $\Delta\omega = 2|\omega_1 - \omega_2|/(\omega_1 + \omega_2)$. By changing the coupling constant C, the synchronization diagram is drawn, which shows dependence of the frequency difference $\Delta\omega$ on the coupling strength.

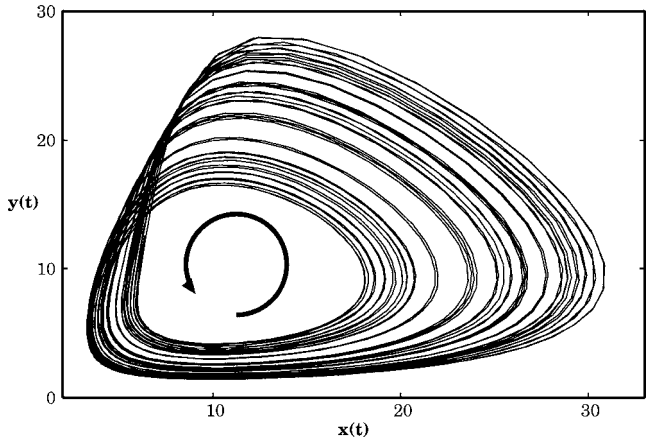

FIG. 6. Chaotic attractor in (x,y)-coordinate space of the predator-prey system (12)–(14).

B. Applications

1. Simulated data

First, we apply our method to simulated data of two interacting chaotic predator-prey systems:[8]

$$\dot{x}_{1,2} = a(x_{1,2} - x_0) - \alpha x_{1,2} y_{1,2}, \tag{12}$$

$$\dot{y}_{1,2} = -b_{1,2} y_{1,2} + \alpha x_{1,2} y_{1,2} - \beta y_{1,2} z_{1,2} + C_{2,1}(y_{2,1} - y_{1,2}), \tag{13}$$

$$\dot{z}_{1,2} = -c(z_{1,2} - z_0) + \beta y_{1,2} z_{1,2}. \tag{14}$$

Each system describes a three trophic food chain, where the basal species x_i is consumed by the predator y_i, which itself is preyed upon by the top predator z_i. In the absence of interspecies interactions, the dynamics is linearly expanded around the steady state $(x_0, 0, z_0)$ with coefficients a, b_i, and c. Predator-prey interactions are introduced via mass-action terms with strength α and β. The asymmetry of the coupling $C_{1,2} = C(1 \mp \chi)$ can be controlled by the asymmetry parameter χ $(-1 \le \chi \le 1)$. Other parameter values were chosen as $a=1$, $c=10$, $x_0=1.5$, $z_0=0.01$, $\alpha=0.1$, $\beta=0.6$, $b_1=1$, $b_2=0.96$.

Under this parameter setting, the predator-prey system generates a phase-coherent chaos, where the trajectory rotates with a nearly constant frequency in the (x_i, y_i) plane but with a chaotic property that appears as irregular spikes in the top predator z_i (see Fig. 6). Because of the phase coherent property, the phase can be well defined for the chaotic attractor, where the unit phase of 2π is defined as a duration between a local maximum of the first component x and the

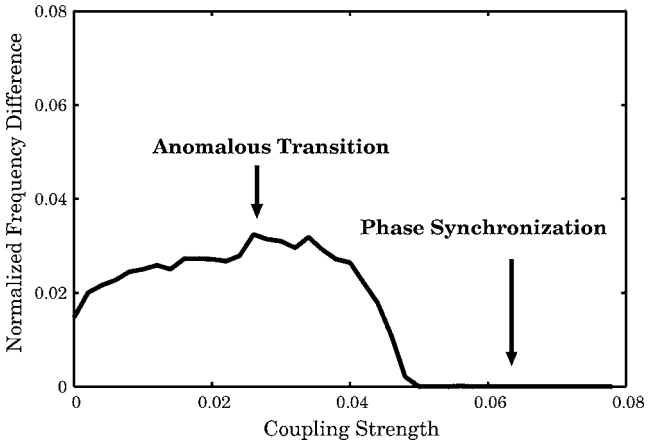

FIG. 7. Dependence of the normalized frequency difference $\Delta\omega$ between the coupled predator-prey systems on the coupling strength $C \in [0, 0.08]$. The coupling asymmetry is set as $\chi=0.1$.

following one. Figure 7 shows the synchronization diagram, which indicates dependence of the frequency difference $\Delta\omega$ between the chaotic oscillators on the coupling strength C in the case of $\chi=0.1$. In the weak coupling regime, chaotic oscillators are not phase synchronized as indicated by the finite amount of the frequency difference. As the coupling strength is increased, the frequency difference initially increases and then for $C>0.034$ it decreases monotonically. As the coupling strength is further increased, the frequency difference becomes zero at $C\approx 0.05$, where the PS sets in. This indicates a clear APS. In a similar manner as the coupled limit cycles [Eqs. (6) and (7)], the anomalous property can be more pronounced by increasing the coupling asymmetry χ.

Let us apply our modeling technique to this simulated system. As the measurement data, two sets of bivariate time series $\{x_1, x_2\}$ were recorded under a no-coupling condition ($C=0$) as well as under a weak coupling condition ($C=0.02$). For each data set, $N=200$ data points were collected with a sampling interval of $\Delta t=0.4$. Following the modeling procedure (B1), the embedding dimension and the time lag were set as $d=3$ and $\tau=1.6$. As the nonlinear model in the procedure (B2), a pair of neural networks $F_{1,2}$, each of which has six units in the input layer, eight units in the middle layer, and three units in the output layer, was utilized. In the ensemble modeling procedure (B3), $Q=5$ sets of the neural networks were averaged to provide the nonlinear function $\bar{F}_{1,2}$.

Figure 8 shows simultaneous drawing of the synchronization diagrams of the predator-prey system (12)–(14) and the nonlinear model. In the case that the asymmetry is not too strong [Figs. 8(a) and 8(b): $\chi=0.1, 0.2$], the model predicts the onset point of PS very precisely. Although the model curve is slightly deviated from the original, the anomalous structure discernible in the original synchronization diagram has been very well recovered by the model. Taking into account the fact that only two data sets were utilized, these results demonstrate the strength of the present modeling technique. It should be noted, however, that in the case that the asymmetry becomes very strong [Fig. 8(c): $\chi=0.6$], the model reconstruction becomes rather unstable. It has been known that as the asymmetry is more strengthened the anomalous structure becomes more pronounced, which induces a much more abrupt transition to PS.[8] The present results imply that it may not be so simple for the nonlinear model to predict such a too sudden change in the synchronization diagram induced by a strongly anomalous system. The nonlinear modeling technique should be reliable under the condition that the anomalous property is moderate.

To study the influence of noise on the reconstruction results, zero-mean Gaussian noise was added to the bivariate data $\{x_1(t), x_2(t)\}$ as observational noise. The asymmetry parameter was set to $\chi=0.1$. To reduce the noise effect, a moving average filter, $x_i'(n\Delta t)=(1/3)\Sigma_{j=1}^{3} x_i((n+j)\Delta t)$ $(i=1,2)$, was applied before the delay coordinate embedding. Figures 8(d) and 8(e) show the results of reconstructing the synchronization diagram under the noise levels of 20% and 30%. Although the reconstructed diagram looks rather different from the original one for the very strong noise level of 30%, the model reconstruction is still quite accurate up to the noise level of 20%, where the anomalous structure is well reproduced with a good prediction on the onset point of the synchronization. This demonstrates the robustness of the present approach against observational noise.

2. Experimental data

Let us apply our method to experimental data from two diffusively coupled nonidentical Chua circuits, which are known to be a good experimental representative of APS.[9,10] From the experimental setup explained in detail in Ref. 10, bivariate time series $\{\xi_1(t), \xi_2(t)\}$ were measured from both of the coupled circuits with a sampling frequency of 25 kHz. The coupling strength is scaled as $C=1/R_C$ using a resistance R_C that connects the two Chua circuits. Figure 9 shows the synchronization diagram observed from the experiment. As the coupling strength is increased, the frequency difference between the coupled circuits increases initially, representing a clear anomalous structure until $C<8.4\times10^{-6}$. The PS regime then appears in $C\in[8.4\times10^{-6}, 1.68\times10^{-5}]$. This interval of zero frequency difference corresponds to an antiphase regime. As the coupling is further increased $C>1.68\times10^{-5}$, desynchronization of coupled oscillators appears. For very large coupling, this desynchronization regime disappears with the onset of in-phase synchrony. Details of the in-phase synchrony are described in Ref. 10, which is beyond the scope of the present study. We limit our attention here to identify the anomalous structure only.

Following the modeling procedures of (B1)–(B4), which were applied to the experimental data, the embedding dimension and the time lag were set as $d=3$ and $\tau=1.2\times10^{-4}$ s. As the nonlinear model $F_{1,2}$, a pair of neural networks, having six units in the input layer, eight units in the middle layer, and three units in the output layer, was exploited. To make the modeling more reliable, the ensemble model $\bar{F}_{1,2}$ was constructed from $Q=10$ different realizations of the neural networks. We have studied the following three cases: (a) modeling two data sets with $R_C=339$ kΩ and 229 kΩ, (b) modeling two data sets with $R_C=339$ kΩ and 129 kΩ, and (c) modeling two data sets with $R_C=169$ kΩ and 59.25 kΩ.

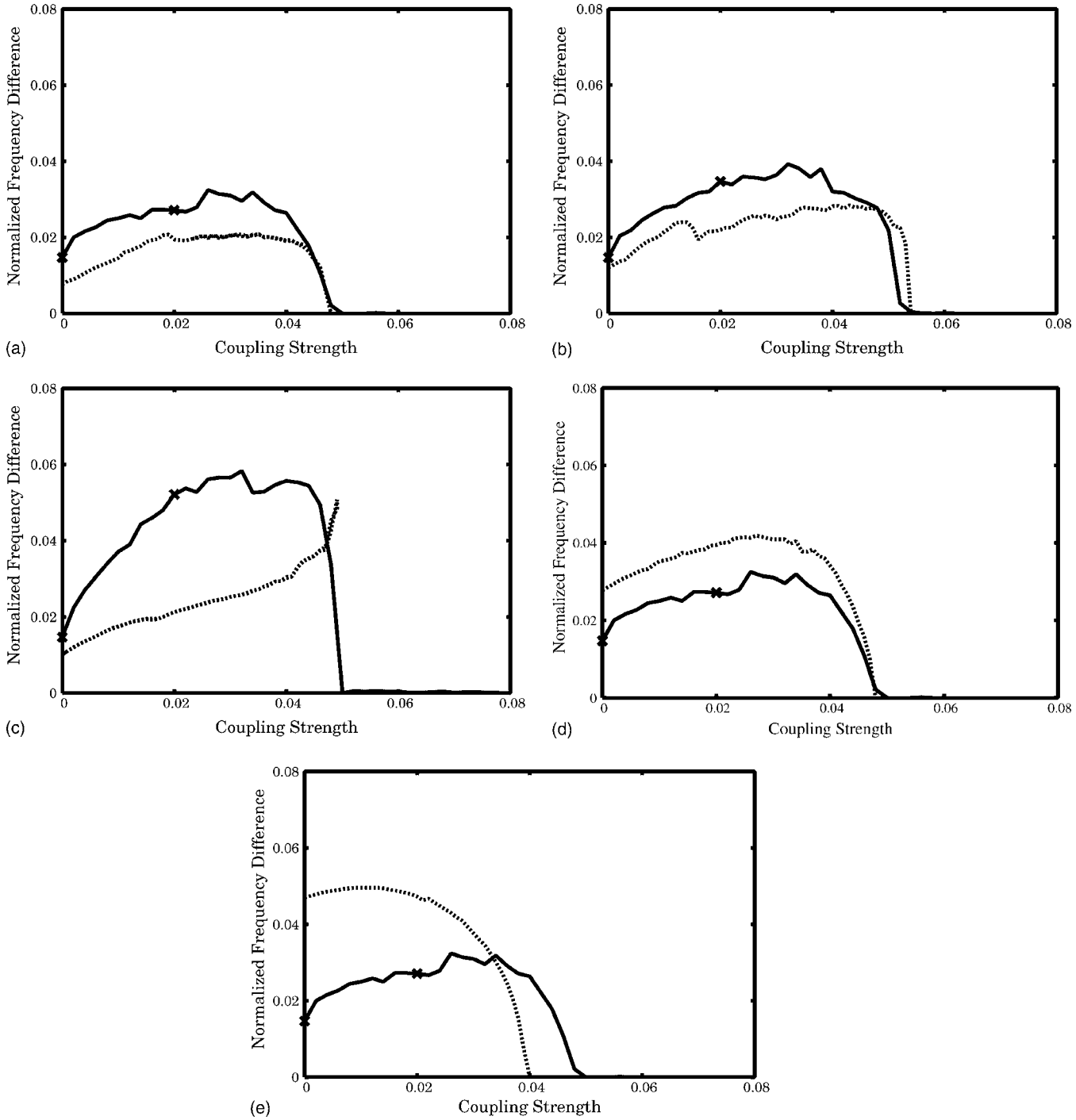

FIG. 8. Synchronization diagrams are drawn for two coupled predator-prey system (solid line) and its nonlinear model (dotted line). Normalized frequency difference $\Delta\omega$ is plotted by changing the coupling strength $C \in [0, 0.08]$. Locations of the data used for the modeling are indicated by the cross marks. (a) χ=0.1, (b) χ=0.2, (c) χ=0.6, (d) χ=0.1 with 20% observational noise, and (e) χ=0.1 with 30% observational noise.

Figure 10 shows simultaneous drawing of the synchronization diagrams of the experimental system and the nonlinear model. In the case (a), the nonlinear model does not show any transition to PS within $C \in [0, 1.8 \times 10^{-5}]$, thus fails to locate the onset point of PS [Fig. 10(a)]. This might be due to the same difficulty as we have seen in the modeling study of the simulated data from the coupled chaotic predator-prey systems. Namely, in the case that the anomalous transition to PS is too abrupt, nonlinear model cannot predict such a sudden change in the synchronization diagram. The situation of the case (a) can be greatly improved in the case (b), where one of the two data sets is located much closer to the PS regime. This helps to locate the onset point of the PS ($C \approx 8.4 \times 10^{-6}$) more precisely. The anomalous structure is, however, still not recovered in this case. Location of the transition from PS to desynchronization ($C \approx 1.5 \times 10^{-5}$) is also not very accurate. The case (c) represents the best reconstruction, which very precisely locates the onset point of the PS ($C \approx 8.4 \times 10^{-6}$), as well as the transition point to the desynchronization ($C \approx 1.68 \times 10^{-5}$).

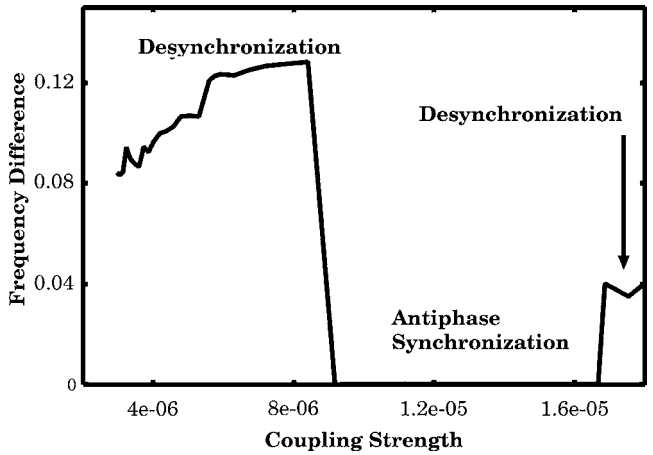

FIG. 9. Synchronization diagram of two diffusively coupled nonidentical Chua circuits. Frequency difference $\Delta\omega$ between the two circuits is plotted against coupling strength $C=1/R_C \in [0, 1.8\times 10^{-5}]$.

Furthermore, the anomalous structure discernible in the experimental system is recovered in this case. This is mainly due to the fact that here the two data records were taken not only from the regime of anomalous transition but also from the regime of desynchronization on the other side of the synchronization diagram. Compared with the cases (a) and (b), which attempt an extrapolation of the synchronization diagram by using only one sided data sets, the case (c) attempts an interpolation by using the both-sided data sets. It is reasonable that such a rich global information on the two distinct types of the nonsynchronized dynamics is of great help for recovering the synchronization diagram.

IV. CONCLUSIONS AND DISCUSSION

Modeling techniques have been presented for detecting the anomalous structure of two coupled nonlinear oscillators from time series data. We have dealt with both coupled limit cycle oscillators and coupled chaotic oscillators. Two approaches were presented: (i) phase equational modeling of coupled limit cycle oscillators and (ii) nonlinear predictive modeling of coupled chaotic oscillators. By using simulated data from two coupled limit cycle predator-prey system, the phase equation model was shown to be capable of recovering the synchronization diagram including the anomalous structure from only a single bivariate data set. The onset point of PS was well predicted by the model. Interaction functions as well as natural frequencies of the two limit cycles were also estimated with a good precision.

A nonlinear modeling technique was then applied to simulated data from two interacting chaotic predator-prey systems and also to experimental data from two coupled Chua circuits. In the case in which the anomalous structure was moderate and the transition from non-PS to PS was not too abrupt, the nonlinear model was capable of recovering the synchronization diagram from only two sets of measurement data associated with different coupling strength. The onset point of PS was precisely predicted and the anomalous transition was well reproduced. The nonlinear model, however, failed to recover the synchronization diagram as the anomalous structure got more pronounced and the transition to PS became too abrupt. This difficulty can be overcome by utilizing data sets from nonsynchronized regimes located on both sides of PS. Application to the coupled Chua circuits showed that the experimental synchronization diagram was well recovered, if the data sets are taken from both sides of PS, although the experimental system has a rather sharp anomalous structure. This improvement is reasonable, since in this case the recovery corresponds to the interpolation of the synchronization diagram. Hence, it is concluded that the modeling data are preferred to be taken not only from one

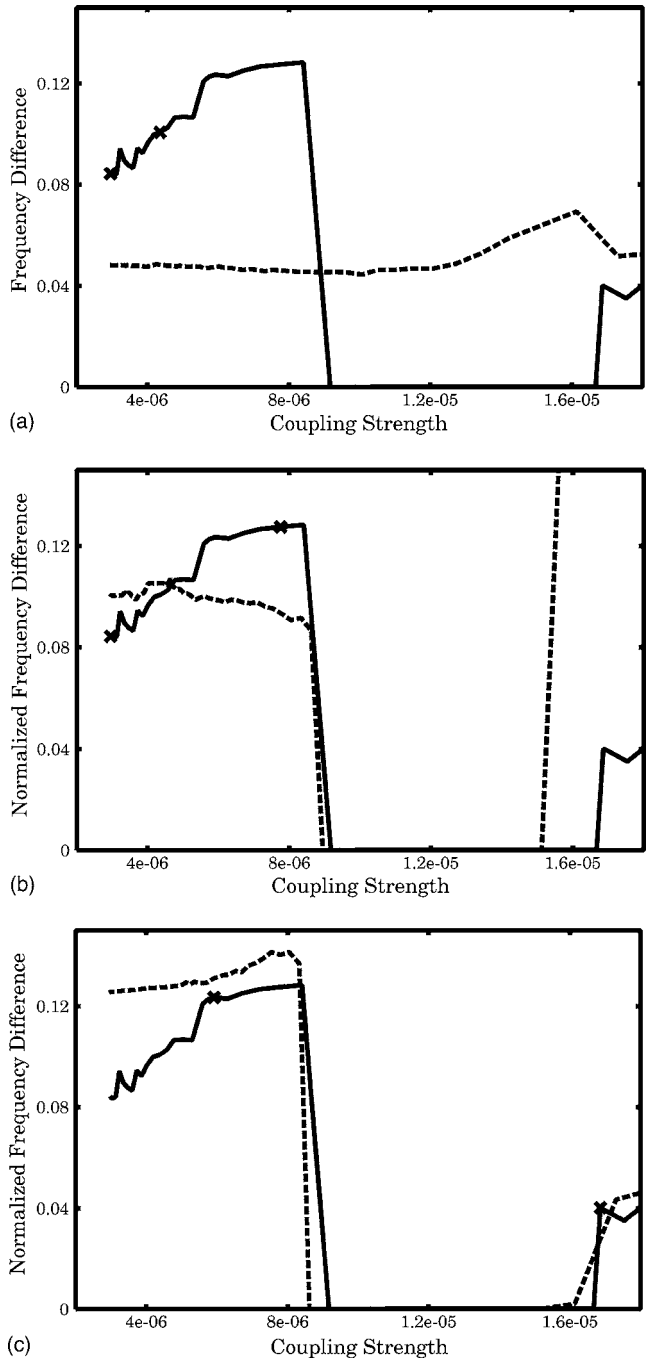

FIG. 10. Synchronization diagram of the experimental system (solid line) and the model prediction (dotted line). Locations of the data used for the modeling are indicated by the crosses. (a) Data from R_C=339 kΩ, 229 kΩ. (b) Data from R_C=339 kΩ, 129 kΩ. (c) Data from R_C=169 kΩ, 59.25 kΩ.

side but from both sides of the PS regime whenever such data are available.

This kind of modeling approach should be of significant importance for studying synchronization of biological systems such as firing neurons or ecological systems. In particular, we have used the predator-prey model as a typical example of APS. In the context of ecology, it has been known that asynchrony of fluctuating animal populations might be important for increasing the chances of global persistence, since asynchrony can spread the survival risk in a fluctuating environment.[32,33] Synchronization, on the other hand, tends to increase the risk of global species extinction. Therefore, anomalous structure in a weak coupling regime before the onset of synchronization may play an important role in ecology, although further careful investigations from both theory and experiment are awaited. The present methodology requires measurements of coupled oscillators from a weak coupling regime that gives rise to asynchronous dynamics. This requirement would fit to some population data, where asynchrony is essential for lowering the extinction risk. Concerning the effect of noise, which is inherent in ecological data, the present approach was shown to be robust up to 20% level of observational noise. Although the measurements from nature can exceed this level, the present approach may have a chance to recover an overall structure of the anomalous transition, thereby the onset point of synchronization can be approximately predicted. It should be finally noted that, in order for the application to ecology, the present approach should be further extended to the case of spatially distributed oscillators, since the spatial structure plays a key role in ecological systems. Such an extension will be considered in a future study.

ACKNOWLEDGMENTS

I.T.T. was supported by the research fellowship of the Alexander-von-Humboldt Foundation and by Grant-in-Aid for Scientific Research (No. 20560352) of the Japan Society for the Promotion of Science (JSPS). S.K.D was supported by the DST, India under Grant No. SR/S2/HEP-03/2005. J.K. was supported by SFB 555 (DFG). A part of this study was supported by SCOPE (071705001) of Ministry of Internal Affairs and Communications (MIC), Japan.

[1] A. T. Winfree, *The Geometry of Biological Time* (Springer, New York, 1980).
[2] Y. Kuramoto, *Chemical Oscillations, Waves and Turbulence* (Springer, Berlin, 1984).
[3] A. Pikovsky, M. Rosenblum, and J. Kurths, *Synchronization - A Universal Concept in Nonlinear Sciences* (Cambridge University Press, Cambridge, 2001).
[4] M. G. Rosenblum, A. S. Pikovsky, and J. Kurths, Phys. Rev. Lett. **76**, 1804 (1996).
[5] J. Kurths, Ed., Special Issue, Int. J. Bifurcation Chaos Appl. Sci. Eng. **10-11** (2000).
[6] S. Boccaletti, J. Kurths, G. Osipov, D. L. Valladares, and C. Zhou, Phys. Rep. **366**, 1 (2002).
[7] B. Blasius, E. Montbrio, and J. Kurths, Phys. Rev. E **67**, 035204R (2003).
[8] B. Blasius, Phys. Rev. E **72**, 066216 (2005).
[9] S. K. Dana, B. Blasius, and J. Kurths, AIP Conf. Proc. **742**, 69 (2004).
[10] S. K. Dana, B. Blasius, and J. Kurths, Chaos **16**, 023111 (2006).
[11] C. Schafer, M. G. Rosenblum, J. Kurths, and H.-H. Abel, Nature (London) **392**, 239 (1998).
[12] P. Tass, M. G. Rosenblum, J. Weule, J. Kurths, A. S. Pikovsky, J. Volkmann, A. Schnitzler, and H. J. Freund, Phys. Rev. Lett. **81**, 3291 (1998).
[13] N. B. Janson, A. G. Balanov, V. S. Anishchenko, and P. V. E. McClintock, Phys. Rev. Lett. **86**, 1749 (2001).
[14] N. Marwan, M. Romano, M. Thiel, and J. Kurths, Phys. Rep. **438**, 237 (2007).
[15] I. T. Tokuda, J. Swati, I. Z. Kiss, and J. L. Hudson, Phys. Rev. Lett. **99**, 064101 (2007).
[16] E. Baake, M. Baake, H. G. Bock, and K. M. Briggs, Phys. Rev. A **45**, 5524 (1992).
[17] M. Stone, J. R. Stat. Soc. Ser. B (Methodol.) **36**, 111 (1974).
[18] H. Sakaguchi, S. Shinomoto, and Y. Kuramoto, Prog. Theor. Phys. **77**, 1005 (1987).
[19] I. Z. Kiss, Y. M. Zhai, and J. L. Hudson, Phys. Rev. Lett. **94**, 248301 (2005).
[20] I. Tokuda, J. Kurths, and E. Rosa Jr., Phys. Rev. Lett. **88**, 014101 (2002).
[21] I. Tokuda, J. Kurths, E. Allaria, R. Meucci, S. Boccaletti, and F. T. Arecchi, Phys. Rev. E **70**, 035204R (2004).
[22] F. Takens, Lect. Notes Math. **898**, 366 (1981).
[23] T. Sauer, J. A. York, and M. Casdagli, J. Stat. Phys. **65**, 579 (1991).
[24] J. D. Farmer and J. J. Sidorowich, Phys. Rev. Lett. **59**, 845 (1987).
[25] J. P. Crutchfield and B. S. McNamara, Complex Syst. **1**, 417 (1987).
[26] M. Casdagli, Physica D **35**, 335 (1989).
[27] D. E. Rumelhart, J. L. McClelland, and the PDP Research Group, *Parallel Distributed Processing* (MIT Press, Cambridge, 1986).
[28] H. Kantz and T. Schreiber, *Nonlinear Time Series Analysis* (Cambridge University Press, Cambridge, 1997).
[29] M. B. Kennel, R. Brown, and H. D. I. Abarbanel, Phys. Rev. A **45**, 3403 (1992).
[30] D. G. Luenberger, *Linear and Nonlinear Programming* (Addison-Wesley, Reading, MA, 1973).
[31] I. Tokuda, U. Parlitz, and J. Kurths, Int. J. Bifurcation Chaos Appl. Sci. Eng. **17**, 3557 (2007).
[32] M. Heino, V. Kaitala, E. Ranta, and J. Lindström, Proc. R. Soc. London, Ser. B **264**, 481 (1997).
[33] D. J. D. Earn, S. A. Levin, and P. Rohani, Science **290**, 1360 (2000).